INTERNATIONAL JOURNAL OF CLIMATOLOGY
Int. J. Climatol. **34**: 3998–4006 (2014)
Published online 25 March 2014 in Wiley Online Library
(wileyonlinelibrary.com) DOI: 10.1002/joc.3984

Royal Meteorological Society

Short Communication

Recent trends in the regime of extreme rainfall in the Central Sahel

G. Panthou,[a,b,c] T. Vischel[a,b,c] and T. Lebel[a,b,c]*
[a] *University of Grenoble Alpes, LTHE, F-38041 Grenoble, France*
[b] *IRD, LTHE, F-38041 Grenoble, France*
[c] *CNRS, LTHE, F-38041 Grenoble, France*

ABSTRACT: Ongoing global warming raises the hypothesis of an intensification of the hydrological cycle, extreme rainfall events becoming more frequent. However, the strong time–space variability of extreme rainfall makes it difficult to detect meaningful trends in the regime of their occurrence for recent years. Using an integrated regional approach, it is shown that over the last 10 years, the Sahelian rainfall regime is characterized by a lasting deficit of the number of rainy days, while at the same time the extreme rainfall occurrence is on the rise. As a consequence, the proportion of annual rainfall associated with extreme rainfall has increased from 17% in 1970–1990 to 19% in 1991–2000 and to 21% in 2001–2010. This tends to support the idea that a more extreme climate has been observed over 2001–2010: this climate is drier in the sense of a persisting deficit of rainfall occurrence compared to 1950–1969, while at the same time there is an increased probability of extreme daily rainfall.

KEY WORDS Sahel; extreme rainfall; hydrological cycle intensification

Received 30 July 2013; Revised 9 December 2013; Accepted 21 February 2014

1. Introduction

In the past 5 years or so, almost all the West African countries have been struck by floods and inundations of unprecedented magnitude. One emblematic instance in this respect are the Niger river floods of 2010 and 2012, which are the two most important floods ever recorded at the Niamey station since the beginning of the observation in 1929, causing heavy casualties to people living close to the river; another instance is the Ouagadougou inundation of 2009, when 263 mm of rain fall in 10 hours killed eight persons, displaced 150 000 people and destroyed the main hospital and other major infrastructures (Sighomnou *et al.*, 2013).

In a recent paper, Di-Baldassarre *et al.* (2010) argued that the augmentation of inundation-related casualties mainly results from the increasing vulnerability of the population. Other authors (Descroix *et al.*, 2009; Seguis *et al.*, 2004) point to land use and land cover changes as being a major factor producing higher run-off coefficients and thus larger river flows, even in a context of lesser rainfall. On the other hand, major flood events cannot occur without heavy rainfall; it is important to study this climatic component of the flood hazard evolution because global warming is expected to intensify the hydrological cycle, a more extreme climate, meaning longer dry spells and higher heavy rainfall (Giorgi *et al.*, 2011). In some regions of the world, premises of such an intensification of the rainfall regime have been documented (Alpert, 2002). However, West Africa is under-represented in studies assessing extreme rainfall trends at the global scale (Alexander *et al.*, 2006; Groisman *et al.*, 2005; Min *et al.*, 2011) and existing studies focusing on extreme rainfall in the region are very few and often of limited scopes (Goula *et al.*, 2012; New *et al.*, 2006). Several reasons may explain this shortcoming, among which the difficulty to access data is likely an important factor. Moreover, evidencing modifications in the climatology of extreme rainfall at regional scale is especially challenging in a monsoon region like West Africa where heavy rainfall is highly variable both in space and time. Thus, the general requirement of collecting a sufficiently large number of long-term rainfall series for detecting meaningful changes over the past decade or so is especially difficult to meet in West Africa because the number of series has to be larger than in regions characterized by a more regular climate and because of the previously mentioned data access limitations.

It is also worth adding that climate models have difficulties to represent complex regional precipitation patterns and are thus of limited reliability when it comes to detect trends in extreme rainfall regimes. This is even more true for West Africa where recent studies (e.g. Biasutti,

* Correspondence to: T. Lebel, IRD, LTHE, F-38041 Grenoble, France.
E-mail: thierry.lebel@ujf-grenoble.fr

2013; Monerie *et al.*, 2012) establish that the most recent ensemble climate simulations of CMIP5 behave similar to the previous CMIP3 simulations, known for their weakness in reproducing correctly the spatial patterns and multi-decadal variability of the West African rainfall (according to Biasutti, 2013: 'the CMIP5 models stubbornly retain the biases that have plagued previous generation models in this region'). Reproducing correctly the spatial patterns of rainfall intensities and their possible long-term evolution will remain elusive as long as the climate models have difficulties capturing correctly the placement of the Sahel rain band (see, e.g. Cook and Vizy, 2006). Direct observations of rainfall thus stand as the main source of information for such trend detection research. This study consequently seeks to better documenting recent trends in extreme rainfall in West Africa, based on long series of daily rainfall covering the period 1950–2010 quite homogeneously over an extended region in the Central Sahel, a domain shown by Lebel and Ali (2009) to display coherent rainfall fluctuations over the past 60 years. Advanced statistical methods are used to robustly analyse regional trends in the series.

The recent climate of the West African Sahel is characterized by a succession of three periods of roughly equal duration: a wet period [P_1] from 1950 to 1969; a severe dry period [P_2] from 1970 to 1990, known to be the largest climatic signal ever recorded over such a large area since the existence of rain gauge networks (Dai *et al.*, 2004); and finally, the recent period [P_3], from 1991 to 2010, has seen a partial rainfall recovery, albeit with a contrasted pattern (Lebel and Ali, 2009). This strong decadal variability raises two interlaced questions that are addressed in the present paper. The first relates to the effect of the big regional drought on the occurrence of heavy rainfall in the 1970s and 1980s. The second is whether in the recent period – where total annual rainfall is getting closer to the long-term average of the 20th century (see e.g. Nicholson, 2001) – the occurrence and intensity of extreme rainfall are returning to what was observed before the drought. This comes down to investigating the complex relation existing between the variability of the average rainfall regime and the variability of the extremes, which is of far larger amplitude; for instance, the torrential daily rainfall of 263 mm recorded in Ouagadougou in 2009 accounts for almost 30% of the annual total of that year (896 mm), while in 1962, the annual daily maximum (93 mm) accounted for less than 8% of the recorded annual total of 1183 mm. This illustrates that extreme events can appear in dry or moderately wet years, while extremely wet years can happen without any extreme rainy event being recorded.

2. Region and period of study

2.1. Rainfall data

The core of the data used comes from a work undertaken under the support of CIEH (Centre Inter-états d'Etudes Hydrauliques) in the mid-1980s. This allowed pooling the data from more than 700 stations since their starting date of operation. Much of West Africa was covered by this data set, albeit not in a homogeneous way, the coverage being less dense in Nigeria and Guinea, for instance. A complementary work by Le Barbé *et al.* (2002) led to extend in time a large number of series, so that the whole critical period 1950–1990 could be covered. Access to daily rainfall for recent years is especially difficult in West Africa. For the 1990–2010 period, some of these series have been completed (provided by National Meteorological Services of Benin, Burkina Faso and Niger). Altogether, this led us to select for this research on extreme rainfall an area extending from 5°W to 7°E and 9.5°N to 15.5°N. Following a thorough data quality check – consisting in a day-by-day spatial coherency check and the analysis of the complete and extreme daily rainfall distributions, 43 stations having operated continuously from 1950 to 2010 within this area have been selected.

2.2. Climatological context

Figure 1 illustrates the difficulty of diagnosing a possible change in the regime of extremes, when looking at individual stations. It compares the annual rainfall and extreme rainfall occurrence averaged over the wet period P_1 to their counterparts for the last 10 years. The mean annual rainfall displays a coherent spatial signal, with a clear overall latitudinal gradient (average deficit of 80 mm north to 14°N against an average deficit of 140 mm south to 11°N); the persistence of a stronger deficit in the West of the domain, as first analysed by Ali and Lebel (2009) and Lebel and Ali (2009) and more recently by Biasutti (2013), is also visible. In relative values, the average deficit for 2001–2010 compared to 1950–1969 ranges from 20% in the extreme south to 10% in the extreme north. By comparison, the pattern of variation of heavy daily rainfall occurrence between the two periods is very spotty, with stations where the occurrence has increased and stations where it has decreased sometimes at very closed locations. A correlation between the two variables can still be noted as the occurrence of heavy rainfall often decreases in locations where mean annual rainfall decreases by a lot and increases in locations with more moderate decreases in mean annual rainfall. This stems from the important contribution of heavy precipitation events to the total precipitation. However, the spotty pattern of heavy rainfall variations contrasts with the much smoother spatial distribution of the mean annual rainfall changes, pointing to the necessity of developing specific regional approaches if one is to reach meaningful conclusions with respect to a possible enhancement of rainfall intensities.

3. Tools for a regional approach

The first part of this study compares the decadal-scale evolutions of the annual totals and of the annual maxima of daily rainfall over the past 60 years. A peak over threshold (POT) analysis is then carried out in order to analyse the evolution of the heavy rainfall regime in terms of

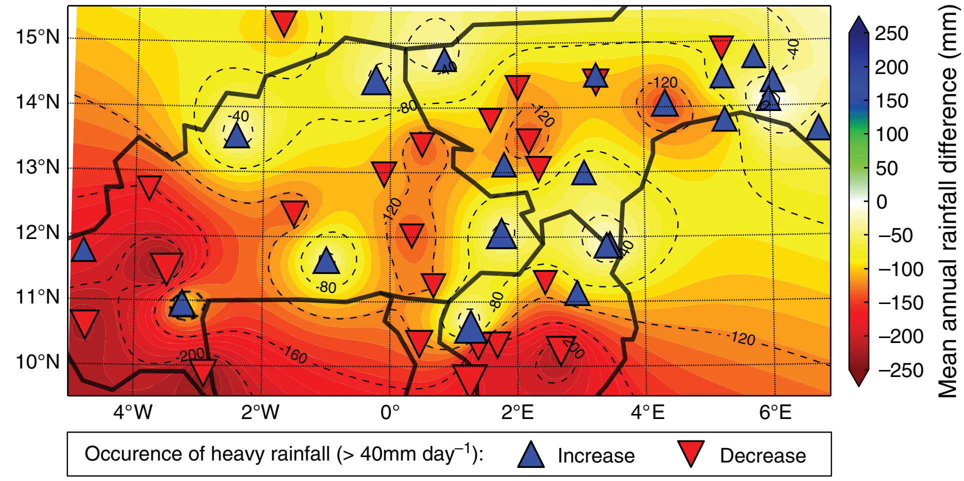

Figure 1. Comparing the annual rainfall and extreme rainfall regimes between the wet period 1950–1969 and 2001–2010. The background map represents the mean annual rainfall differences (obtained by kriging the differences computed at each of the 43 stations), while the triangles indicate an increase (blue, upward) or decrease (red, downward) in the occurrence of daily rainfall over 40 mm day^{-1} at each of the 43 stations. The area of the triangles is proportional to the magnitude of the increase (decrease).

frequency, intensity, percentage of annual rainfall brought by heavy rainfall and number of heavy rainfall days in comparison with the total number of rainy days.

3.1. Standardized precipitation index of annual totals and annual maxima

The standardized precipitation index (SPI) is based on the probability of precipitation for any time scale based on long-term precipitation records. The principle is to fit a probability distribution to the long-term precipitation record and then to transform it to the standard normal distribution that defines the SPI (WMO, 2012). This index is recommended by the World Meteorological Organization in order to detect droughts in rainfall series; it is also a suitable tool for comparing rainfall anomalies at different stations characterized by different means and standard deviations.

3.1.1. SPI for annual totals

The assumption of normality of annual totals being verified in the study area (not shown here) for annual totals the SPI can be simply computed as:

$$\mathrm{SPI_{AR}}\,(i) = \frac{r_i - m_{\mathrm{AR}}}{\mathrm{std_{AR}}} \qquad (1)$$

where $\mathrm{SPI_{AR}}(i)$ is the standardized annual rainfall index for year i, r_i is the annual areal rainfall over the region for year i – computed by kriging the $J = 43$ annual point totals – $\mathrm{m_{AR}}$ and $\mathrm{std_{AR}}$ being the mean and standard deviation, respectively, of the annual areal rainfall series.

3.1.2. SPI for annual maxima

A representation of the cumulative distribution function (cdf) F_j of the annual daily rainfall maxima at each station j is obtained from the spatial Generalized Extreme Value (GEV) model proposed by Panthou *et al.* (2012).

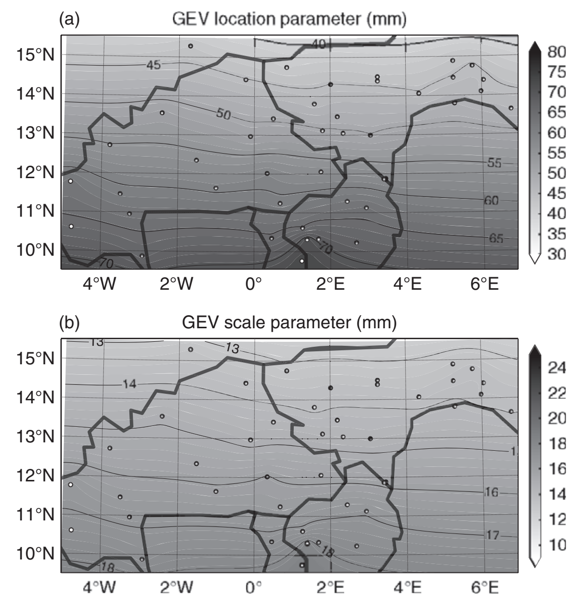

Figure 2. Maps of the location (a) and of the scale (b) parameters of the spatial GEV model fitted to the 43 annual maxima series over the 1950–2010 period using the mean annual rainfall as spatial covariate. The shape parameter is assumed to be constant (equal to 0.06) (Panthou *et al.*, 2012).

This model uses the mean annual rainfall as spatial covariate for the location and the scale parameters (see Figure 2) and assumes the shape parameter to be constant over the whole area (see Appendix A for more explanation). As the GEV model is highly skewed, a standardized index computed directly from the annual maxima would be highly non-symmetrical, making the comparison with $\mathrm{SPI_{AR}}$ difficult.

To get around this difficulty, the annual maximum precipitation index – $\mathrm{SPI_{AM}}$ – is computed in two steps (Min *et al.*, 2011). First for year i, a probability index $f(i)$ is computed:

$$f(i) = \frac{1}{J}\sum_{j=1}^{j=J} F_j\left(z_{ij}\right) \quad (2)$$

where z_{ij} is the annual maximum for year i at station j. The resulting index $f(i)$ fluctuates between two limits: 0 and 1. Its theoretical distribution is by definition uniform and thus symmetrical. Then f is transformed through a standard Gaussian anamorphosis function to obtain the SPI for maxima $\mathrm{SPI}_{\mathrm{AM}}(i)$.

The interannual fluctuations of $\mathrm{SPI}_{\mathrm{AM}}(i)$ are directly comparable to those of $\mathrm{SPI}_{\mathrm{AR}}(i)$, as shown in Figure 3.

3.2. Selecting heavy rainfall through a POT approach

Looking at the time variability of the two indexes $\mathrm{SPI}_{\mathrm{AR}}$ and $\mathrm{SPI}_{\mathrm{AM}}$ provides a global vision of the joint evolution of the annual totals and of the extreme rainfall over the region, showing that (1) their interannual fluctuations are far from coinciding perfectly and (2) they display a different magnitude of the trend over the past 10 years. It should be kept in mind that the fluctuations of these two indices may result from different sources of variability of the underlying rainfall process. In the first work that has ever addressed the link between the rainfall variability at the annual/decadal scales and the variability at the daily scale in West Africa, Le Barbé *et al.* (2002) have shown that the ~200 mm deficit in annual rainfall over 1970–1990 was mostly linked to a large decrease in the occurrence of rainy events, all over West Africa, while the intensity of these rainfall events decreased only slightly and with no consistent spatial pattern. Investigating similar links between the interannual/decadal variability of maximum annual daily rainfall and the occurrence rate/intensity of daily rainfall is not straightforward when looking at individual annual maxima series, due to their much higher sampling variability, compared to that of annual totals.

The POT approach is the most straightforward way to identify whether a long-term change in rainfall annual totals is associated with an increase/decrease in the occurrence of heavy rainfall compared to an increase/decrease in normal rainfall occurrences. This approach also has the advantage of allowing testing the sensitivity of the observed extreme rainfall fluctuations to the threshold used. In a regional context, there are different possibilities for defining this threshold:

i It can be constant for the entire area: typically a value between 20 and 50 mm;
ii It may correspond to a given quantile: typically the 95th or the 99th percentile;
iii It can be defined directly at the regional scale using the regional GEV model proposed by Panthou *et al.* (2012) and by setting a number of events over threshold expected at each station. This method uses the parameter relation between a GEV distribution use in the Block Maxima Analysis (BMA) approach and a P/GP (Poisson/Generalized Pareto) distribution use in a POT approach (see Appendix B).

While all these three approaches were tested, the last approach was finally chosen, because it selects the same number of events at each station, thus guaranteeing a spatial homogeneity of the sampling process – a property that is obviously not guaranteed from the first approach, given the latitudinal gradient of rainfall in this region (at any given level, more events are thus selected in the southern part of the domain than in its northern part). Approach (iii) also protects from the large sampling errors occurring when defining a percentile locally, as in approach (ii).

Two levels of occurrence were chosen in order to define two samples of high rainfall. Extreme rainfall was defined as occurring in average less than 2.5 times per year at any

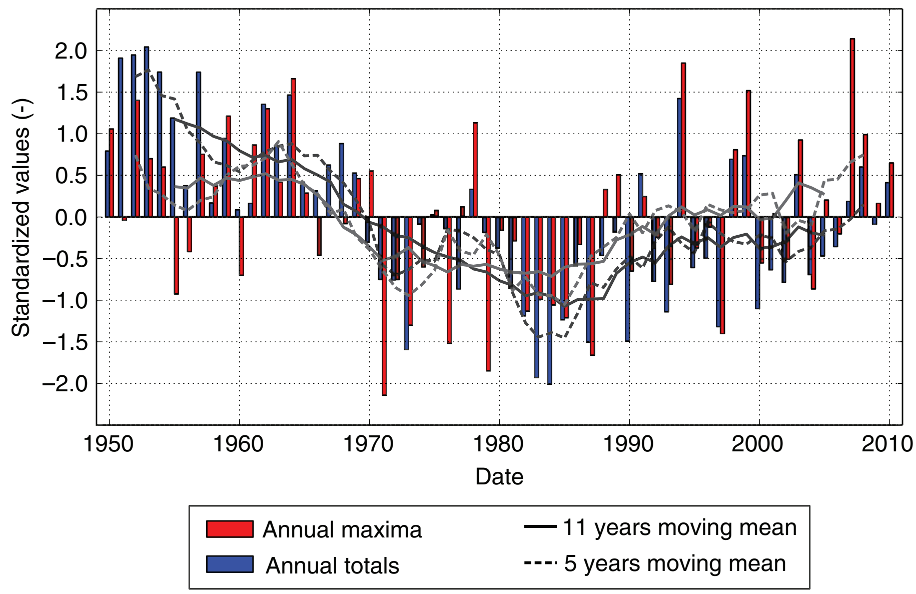

Figure 3. SPIs (a) for the annual totals and (b) for the annual maxima.

station, which is about 100 events per year over our network of 43 stations. Heavy rainfall was defined as occurring in average less than 10 times per year at any station, which is about 400 events per year over our network (this sample of heavy rainfall includes the extreme rainfall). The choice of these two thresholds of occurrence results from a heuristic exploration of daily rainfall thresholds ranging from 10 to 100 mm, and the occurrence rates are averages computed over the whole period of study 1950–2010. Figure 4 shows the areal distribution of the daily rainfall thresholds corresponding to the two selected occurrence rates. The sample of extreme rainfall is made of the daily rainfall larger than a threshold evolving from 30 mm in the north to 60 mm in the south (Figure 4(a)). The sample of heavy rainfall is made of the daily events larger than a threshold evolving from 12 mm in the north to 32 mm in the south (Figure 4(b)).

4. Results

4.1. Standardized indices

Figure 3 displays the two standardized indices for annual totals (blue bars) and annual maxima (red bars), with their corresponding 5- and 11-year moving means. Several key features stem from this graph.

1. After the low values of the annual rainfall and of the annual maxima observed over P_2, the last 20 years (P_3) are characterized by a slow recovery of the annual rainfall, but it remains below the 60-year average (equivalent to a 13% deficit with respect to the wet P1 period, Table 1). Over the same recent period, the 11- and 5-year moving averages of the annual maxima index reach the 60-year average and exceed it substantially after the year 2000, with the two largest values observed in 2007 (2.14) and 1994 (1.85) to be compared to the largest annual value of the wet period (1.66 in 1964).
2. As expected, the interannual variability of the annual maxima index is much larger than for the annual totals, six negative values of SPI_{AM} being observed during the wet years (no negative value of SPI_{AR}) and six positive values of SPI_{AM} being observed during the dry years (only two small positive values of SPI_{AR}).
3. Also worth noting is the fact that the linear coefficient of correlation between the two indices is now larger than during the previous decades (0.17 for P_1, 0.23 for P_2 and 0.76 for P_3).

The POT approach presented in Section 3 will allow further exploring the change observed in the extreme rainfall regime over the last 20 years by looking at a larger set of heavy rainfall than when using the annual maxima only.

4.2. Rainfall intensification in recent years?

The time evolution of various statistics produced by the POT analysis is shown in Figure 5 for the extreme rainfall threshold on the left and for the heavy rainfall threshold on the right.

Figure 5(a) shows the evolution of the occurrence of extreme (respectively heavy) rainfall events from 1950 to 2010. The 11-year moving average curve for the extreme rainfall is very similar to that shown in Figure 3 for the annual maxima, the number of extreme events for the recent years being roughly equal to the number recorded at the beginning of the 1950s that is about 3/year/station. On the contrary, the number of heavy events remains substantially lower (about 11 in recent years – recovering from a minimum of 9 in the 1980s – against about 13 at the beginning of the 1950s). Interestingly, the evolution of the number of heavy rainfall per year is globally similar to that of the annual rainfall: a maximum average deficit over the region of study of about 30% was reached in the mid-1980s and, despite a recovery in recent years, a deficit of about 15% in comparison to the 1950s remains today.

Most worth noting is the fact that the proportion of extreme events in the population of the heavy events, as well as in the population of all the rainy days, has increased over the 2000s, as shown in Figure 5(b) and in Table 1. This stems from the fact that the absolute number of extreme

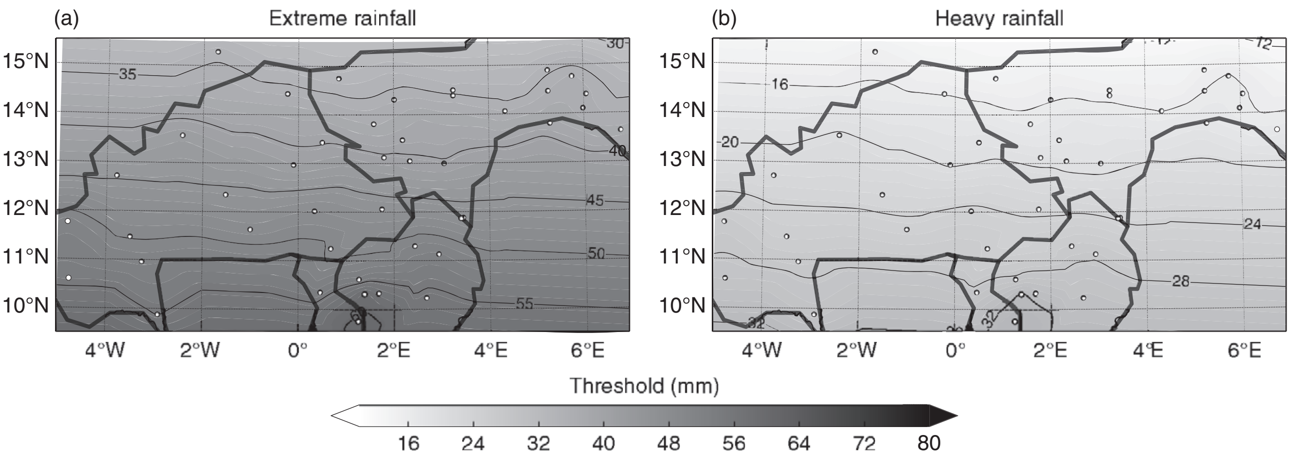

Figure 4. Daily rainfall thresholds used to define (a) extreme rainfall occurring in average less than 2.5 times per year at any given station and (b) heavy rainfall occurring in average less than 10 times per year at any given station.

Table 1. Comparative statistics of the rainfall regime for various periods.

	P1 (1950–1969)	P2 (1970–1990)	P3 (1991–2010)	P3a (1991–2000)	P3b (2001–2010)
Annual rainfall (mm)	850	680	735	730	740
Number of rainy days	62	54	56	56	56
Number of extreme; heavy rainy days	2.9; 12.0	2.1; 9.1	2.6; 10.5	2.4; 10.4	2.8; 10.6
% Extreme; heavy rainy days	5.0; 22.6	4.0; 19.7	5.1; 22.1	4.7; 22.1	5.5; 22.1
% Annual rainfall from extreme rain; from heavy rain	19.0; 55.2	17.0; 52.7	20.0; 56.6	18.9; 56.4	21.2; 56.9

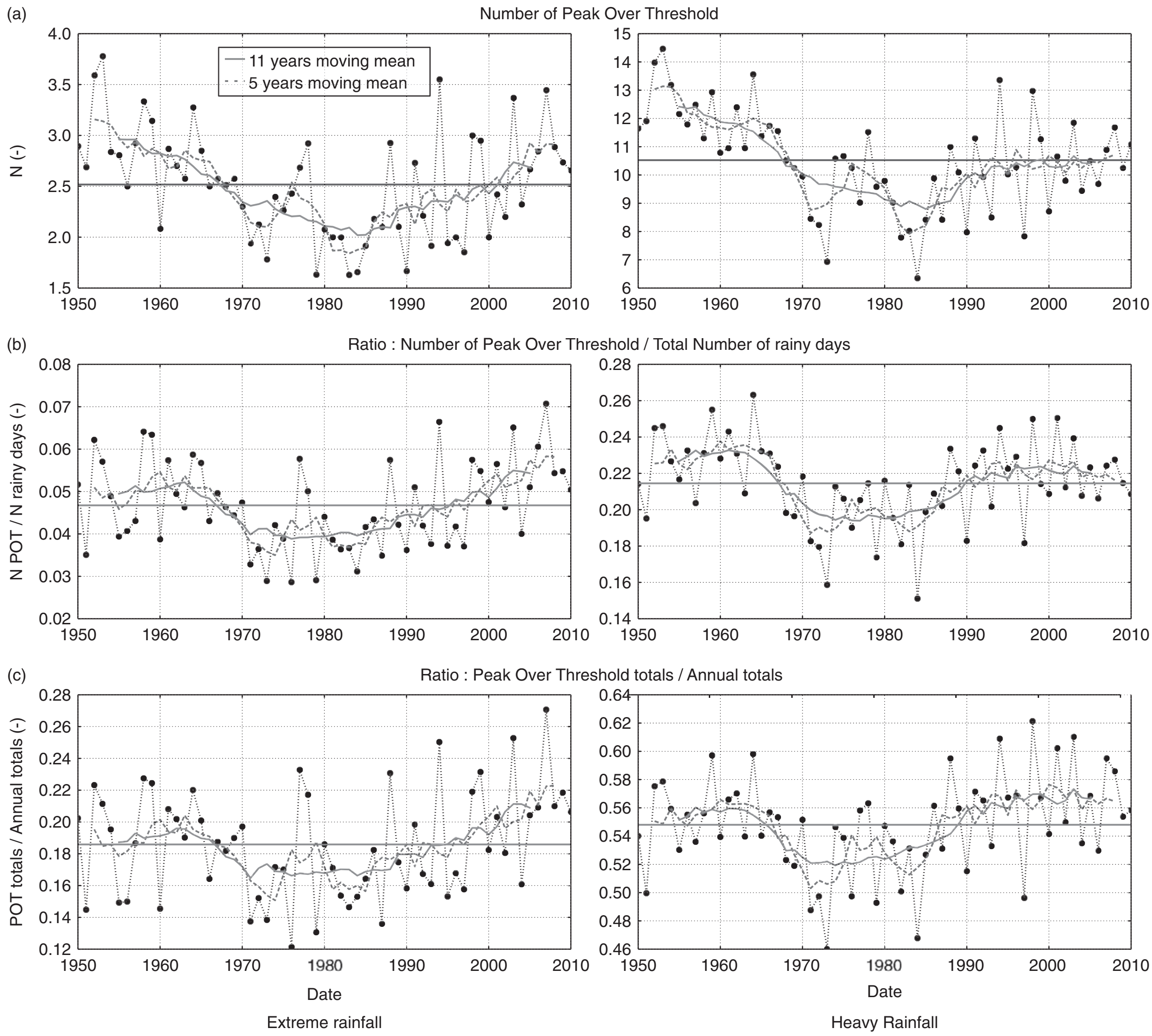

Figure 5. Evolution of the statistics of extreme (left panel) and heavy (right panel) rainfall from 1950 to 2010: (a) number of extreme (heavy) rainfall; (b) percentage of extreme (heavy) rainy days; (c) contribution of the extreme (heavy) rainy days to the annual total.

rainfall events has regained its value observed in the 1950s, while the number of rainy days per year remains 10% below the P_1 average.

As a consequence, the contribution of the extreme (heavy) rainy days in the annual totals has also markedly increased from 19% (55) in the wet period to 21% (57) during the last decade (Figure 5(c) and Table 1).

The statistics given in Table 1 update and refine the previous findings of Le Barbé *et al.* (2002). In average, over our study area, the annual rainfall deficit of the dry period P_2 with respect to the wet period P_1 was 20%; the number of rainy days decreased by 12.9% and the number of extreme rainy days decreased by 28%. This confirms that the main factor of the rainfall deficit during P_2 was a lower occurrence of rainy days and it adds to previous knowledge by evidencing that extreme rainy days were the most affected. By contrast, the recent decade is characterized by a continuing deficit of rain

Table 2. Relative variation of the statistics between the recent decade 2001–2010 and the wet period 1950–1969, along with the corresponding *P*-Values of the T-Student test.

	01–10 versus 50–69	*P* value Student	Significant 1% level	Significant 10% level
Annual rainfall	−12.8%	0.01%	Yes	Yes
Number of rainy days	−10.4%	0.00%	Yes	Yes
Number of heavy rainy days	−11.8%	0.07%	No	Yes
Number of extreme rainy days	−3.4%	55.1%	No	No
Heavy rainy days	−2.1%	46.9%	No	No
Extreme rainy days	+10.4%	14.9%	No	No
Annual rainfall from heavy rain	+3.1%	12.3%	No	No
Annual rainfall from extreme rain	+11.2%	8.5%	No	Yes

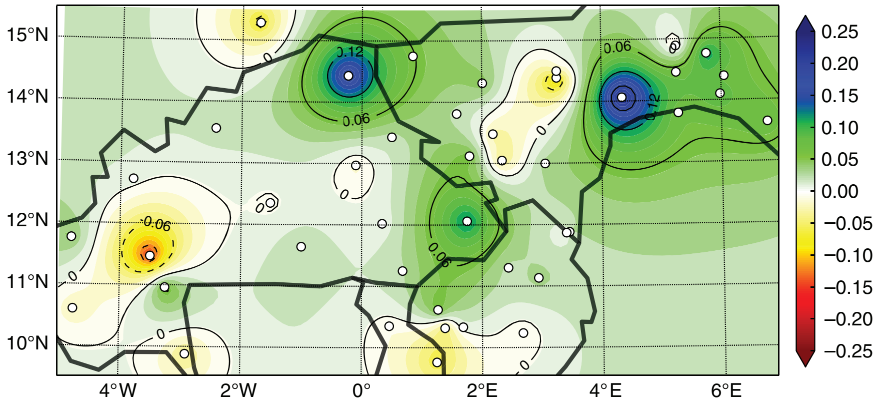

Figure 6. Proportion of the extreme rainfall in the annual totals: map of the absolute differences between the 2001–2010 values and the 1950–1969 values.

occurrence (−9.7% with respect to P_1 and −3% with respect to the P_1+P_2 average), and by a strong recovery in the occurrence of extreme rainfall, which is now at a level comparable to the level of the wet period. This persisting deficit in rainfall occurrence is significant at the 1% level, as shown in Table 2. Altogether, the total rainfall deficit also remains significant as may be seen from the *t*-test values given in Table 2 (−12.8%/P_1 and −2.6%/P_1+P_2 average), while the proportion of the number of extreme rainy days within the total population of rainy days has strongly increased (+10%/P_1 and +22%/P_1+P_2 average).

This picture is characteristic of a higher hydro-climatic intensity as defined by Giorgi *et al.* (2011) with more and/or longer dry spells and a higher probability of heavy rainfall during wet periods, leading to an increasing percentage of annual rainfall due to extreme rainfall.

5. Discussion

Extreme rainfall being highly variable by nature, meaningful conclusions on possible changes in their occurrence and/or intensity cannot be reached by looking at individual stations. The regional approach proposed and applied to the Central Sahel leads us to confidently assert that a more extreme climate has been observed over the last 10 years, with a persisting deficit of the occurrence of rainfall associated with an increase in the occurrence of extreme daily rainfall. In other words, the average intensity of the rainy events has increased, not so much because all rainy events are more intense but because of an increase in the intensity of the largest rainy events. Obviously, this raises the important additional question of how this recent decadal scale trend is linked to either large-scale changes in the atmospheric circulation or more local factors enhancing the convection intensity or both. Figure 6 may contribute to that discussion by showing that the increase in the weight of the extreme rainfall in the annual totals is greater in the north than in the south: from 21% over 1950–1969 to 25% over 2001–2010, north to 13°N, from 18 to 20%, between 11°N and 13°N, from 17 to 18%, south to 11°N. These numbers point to a stronger intensification of the hydrological cycle in the drier part of our domain of study. Also worth noting is the fact that the intensification is weaker in the Western part of the domain of study, even reaching negative values in south-west Burkina. Monerie *et al.* (2012) have shown that in the CMIP5 runs, the drying of the Western Sahel is persisting, in association with a reinforcement of the descending branch of the Walker cell and a southward migration of the ITCZ during the first part of the rainy season. It would make sense to consider that there is a link between the west-east gradient of intensification and the change of the latitudinal circulation, but it is very difficult to assess the nature of this link. For one, as stated in Section 1, detecting meaningful modification of rainfall intensities in the climate models is plagued by the weakness of their representation of convection. Another route would be to explore whether there is some seasonality in rainfall intensification that could be related to the intraseasonal changes of the atmospheric circulation pointed out by Monerie *et al.* (2012) and Biasutti (2013). The small size of our samples does not yet allow for such a refined analysis but is something that should be considered when more data are made available to the scientific community. Beyond the climatological perspective, the stronger than average increase in both the number of dry spells and the number of extreme rainfall events in the northern areas already characterized by the most erratic rainfall regime has strong implications for the future of crop yields as well of inundations. Assessing these implications requires looking at smaller time scale than the daily scale, which provides a strong incentive to set up and maintain specific long-term observing systems such as the AMMA-CATCH observatory (Lebel *et al.*, 2009).

Acknowledgements

This research was partly funded by Labex OSUG@2020 (ANR10 LABX56), partly by the French National Research Agency (ANR) through the ESCAPE project (ANR-10-CEPL-005) and partly by IRD and INSU through the AMMA-CATCH observing system. Gérémy Panthou, PhD, grant was funded by SOFRECO. This work was made possible thanks to the participation of the National Meteorological Services of Benin, Burkina Faso and Niger.

Appendix A. Regional GEV model

The series of extreme daily rainfall are extracted through the block maxima procedure (Coles, 2001). Let $X_1, \ldots, X_k$ be a sequence of k independent and identically distributed (iid) random variables and $x_1, \ldots, x_k$ are realizations of these random variables. The block maxima approach consists of defining blocks of n observations and to take the maxima within each block. This leads to obtain a vector of $N = k/n$ maxima z (N realizations of the random variable Z):

$$z = \left\{z_1 \ldots z_N\right\} = \left\{\max\left(x_1, \ldots, x_n\right), \max\left(x_{n+1}, \ldots, x_{2n}\right), \ldots \max\left(x_{k-n+1}, \ldots, x_k\right)\right\} \quad \text{(A1)}$$

In this study, each block contains one year of data ($n = 365$ observations) and thus $N = 61$. For each of the 43 stations, a series of 61 annual maximum daily rainfall is extracted from the daily data.

As $X_1, \ldots, X_k$ are iid, $Z_1, \ldots, Z_N$ forms an iid sample of the block maxima variable Z. If n is large enough, the block maxima distribution can be approximated by the GEV distribution (Coles, 2001):

$$G(z; \mu, \sigma, \xi) = \exp\left\{-\left[1 + \xi\left(\frac{z-\mu}{\sigma}\right)\right]^{-1/\xi}\right\} \quad \text{for } z > \mu - \frac{\sigma}{\xi} \quad \text{(A2)}$$

with μ being the location parameter, $\sigma > 0$ the scale parameter and ξ the shape parameter. The shape parameter describes the behaviour of the distribution tail: a positive (respectively negative) shape corresponds to a heavy-tailed (respectively bounded) distribution.

GEV models require that the underlying random variables $X_1, \ldots, X_k$ are independent, or at least short-term dependent (i.e. that they follow Leadbetter's D-condition, Leadbetter, 1974). The short-term dependence of daily rainfall was verified by Ali *et al.* (2006) and Gerbaux *et al.* (2009). The independence of block maxima is ensured by working on annual daily rainfall maxima.

Panthou *et al.* (2012) recently proposed a regional statistical model of extreme rainfall over West Africa. The principle of the model is to gather all station data in one unique sample and to fit the GEV parameters by incorporating spatial covariates. As the GEV model incorporates a spatial covariate, Z becomes Z_j, where Z_j is the annual maximum daily precipitation series at station j. The spatial covariate at station j will be denoted s_j . Among the different spatial covariates tested, Panthou *et al.* (2012) have shown that the mean annual rainfall was the most appropriate to represent the pattern of both the location (μ) and the scale (σ) parameters over the study area, ξ being supposed uniform:

$$Zj \sim \text{GEV}\left\{\mu\left(s_j\right), \sigma\left(s_j\right), \xi\right\} \quad \text{(A3)}$$

where μ and σ are linear functions of s:

$$\mu(s) = \mu_0 + \mu_1 \times s \text{ and } \sigma(s) = \sigma_0 + \sigma_1 \times s \quad \text{(A4)}$$

The stationary regional GEV model is fitted over the whole study period according to the maximum likelihood function:

$$l(\theta) = \sum_{j=1}^{j=J}\sum_{t=1}^{t=N} \log\left\{g\left[z_j; \mu\left(s_j\right), \sigma\left(s_j\right), \xi\right]\right\} \quad \text{(A5)}$$

where θ denotes the vector of the five GEV parameters (μ_0, μ_1, σ_0, σ_1, ξ) and g the GEV density function.

Figure 2 shows the maps of the two GEV parameters, $\mu(s)$, $\sigma(s)$. As they are conditioned by the same spatial covariate, their pattern is similar.

Appendix B. Point process: from BMA-GEV to POT-P/GP

The extreme value theory (Coles, 2001) proposes two approaches to extract extreme samples and the corresponding statistical models to describe the tail of one distribution: The GEV model is the appropriate model to describe Block Maxima samples (as described below) and the GP (Generalized Pareto) is the appropriate model to describe POT samples.

The extreme value theory proposes a relation between the two approaches called the point process (Coles, 2001; Madsen *et al.*, 1997). The point process proposes a relation between the parameters of a P/GP (Poisson/Generalized Pareto) model and GEV model. The P/GP model has four parameters: λ (mean occurrence rate of POT during a block of length n), τ (threshold value), α (scale parameter) and ξ (shape parameter).

This relation is (GEV parameters on the left, P/GP on the right):

$$\mu = \tau - \frac{\alpha}{\xi}\left(1 - \lambda^{\xi}\right) \tag{B1}$$

$$\sigma = \alpha\lambda^{\xi} \tag{B2}$$

$$\xi = \xi \tag{B3}$$

By replacing α in Equation (B1), we can obtain a threshold value (τ) for a given occurrence rate during a block n (λ) from the three parameters of the GEV:

$$\tau = \mu + \frac{\sigma}{\xi\lambda^{\xi}}\left(1 - \lambda^{\xi}\right) \tag{B4}$$

Spatial thresholds in Figure 4 are thus obtained using the spatial parameters of the regional GEV model (Appendix A) and by fixing λ to 2 and 10.

References

Alexander LV, Zhang X, Peterson TC, Caesar J, Gleason B, Haylock M, Collins D, Trewin B, Rahimzadeh F, Tagipour A, Rupa Kumar K, Revadekar J, Griffiths G, Vincent L, Stephenson DB, Burn J, Aguilar E, Brunet M, Taylor M, New M, Zhai P, Rusticucci M, Vazquez-Aguirre JL. 2006. Global observed changes in daily climate extremes of temperature and precipitation. *J. Geophys. Res.* **111**: D05109.

Ali A, Lebel T. 2009. The Sahelian standardized rainfall index revisited. *Int. J. Climatol.* **29**(4): 1705–1714.

Ali A, Amani A, Lebel T, Ibrahima S. 2006. Utilisation optimale de l'information pluviométrique des MCGA aux échelles hydrologiques au Sahel = Optimal use of GCM rainfall information at the hydrological scale in the Sahel. In *Climate Variability and Change: (Hydrological Impacts)*. Presented at the Fifth FRIEND, International association of hydrological sciences press, Wallingford, ROYAUME-UNI. Havana, Cuba, 430–435.

Alpert P. 2002. The paradoxical increase of Mediterranean extreme daily rainfall in spite of decrease in total values. *Geophys. Res. Lett.* **29**: 1–4.

Biasutti M. 2013. Forced Sahel rainfall trends in the CMIP5 archive. *J. Geophys. Res.: Atmos.* **118**: 1613–1623, DOI: 10.1002/jgrd.50206.

Coles S. 2001. *An Introduction to Statistical Modeling of Extreme Values*. Springer: London.

Cook KH, Vizy EK. 2006. Coupled model simulations of the West African monsoon system: twentieth- and twenty-first-century simulations. *J. Clim.* **19**(15): 3681–3703, DOI: 10.1175/JCLI3814.1.

Dai A, Lamb PJ, Trenberth KE, Hulme M, Jones PD, Xie P. 2004. The recent Sahel drought is real. *Int. J. Climatol.* **24**: 1323–1331.

Descroix L, Mahé G, Lebel T, Favreau G, Galle S, Gautier E, Olivry JC, Albergel J, Amogu O, Cappelaere B, Dessouassi R, Diedhiou A, Le Breton E, Mamadou I, Sighomnou D. 2009. Spatio-temporal variability of hydrological regimes around the boundaries between Sahelian and Sudanian areas of West Africa: A synthesis. *J. Hydrol.* **375**: 90–102.

Di-Baldassarre G, Montanari A, Lins H, Koutsoyiannis D, Brandimarte L, Blöschl G. 2010. Flood fatalities in Africa: from diagnosis to mitigation. *Geophys. Res. Lett.* **37**: 1–5.

Gerbaux M, Hall N, Dessay N, Zin I. 2009. The sensitivity of Sahelian runoff to climate change/Sensibilite au changement climatique du ruissellement au Sahel. *Hydrolog. Sci. J.* **54**: 5–16.

Giorgi F, Im E-S, Coppola E, Diffenbaugh NS, Gao XJ, Mariotti L, Shi Y. 2011. Higher hydroclimatic intensity with global warming. *J. Clim.* **24**: 5309–5324.

Goula BTA, Soro EG, Kouassi W, Srohourou B. 2012. Tendances et ruptures au niveau des pluies journalières extrêmes en Côte d'Ivoire (Afrique de l'Ouest). *Hydrolog. Sci. J.* **57**: 1067–1080.

Groisman PY, Knight RW, Easterling DR, Karl TR, Hegerl GC, Razuvaev VN. 2005. Trends in intense precipitation in the climate record. *J. Clim.* **18**: 1326–1350.

Le Barbé L, Lebel T, Tapsoba D. 2002. Rainfall variability in West Africa during the years 1950-90. *J. Clim.* **15**: 187–202.

Leadbetter M. 1974. On extreme values in stationary sequences. *Probab. Theory Relat. Fields* **28**: 289–303.

Lebel T, Ali A. 2009. Recent trends in the Central and Western Sahel rainfall regime (1990–2007). *J. Hydrol.* **375**: 52–64.

Lebel T, Cappelaere B, Galle S, Hanan N, Kergoat L, Levis S, Vieux B, Descroix L, Gosset M, Mougin E, Peugeot C, Séguis L. 2009. AMMA-CATCH studies in the Sahelian region of West-Africa: an overview. *J. Hydrol.* **375**: 3–13.

Madsen H, Rasmussen PF, Rosbjerg D. 1997. Comparison of annual maximum series and partial duration series methods for modeling extreme hydrologic events 1. At-site modeling. *Water Resour. Res.* **33**: 747–757.

Min SK, Zhang X, Zwiers FW, Hegerl GC. 2011. Human contribution to more-intense precipitation extremes. *Nature* **470**: 378–381.

Monerie PA, Fontaine B, Rocou P. 2012. Expected future changes in the African monsoon between 2030 and 2070 using some CMIP3 and CMIP5 models under a mediup-low RCP scenario. *J. Geophys. Res.* **117**: D16111, DOI: 10.1029/2012JD017510.

New M, Hewitson B, Stephenson DB, Tsiga A, Kruger A, Manhique A, Gomez B, Coelho CA, Masisi DN, Kululanga E *et al.* 2006. Evidence of trends in daily climate extremes over southern and West Africa. *J. Geophys. Res.* **111**: D14102.

Nicholson SE. 2001. Climatic and environmental change in Africa during the last two centuries. *Clim. Res.* **17**(2): 123–144.

Panthou G, Vischel T, Lebel T, Blanchet J, Quantin G, Ali A. 2012. Extreme rainfall in West Africa: a regional modeling. *Water Resour. Res.* **48**: 1–19.

Seguis L, Cappelaere B, Milési G, Peugeot C, Massuel S, Favreau G. 2004. Simulated impacts of climate change and land-clearing on runoff from a small Sahelian catchment. *Hydrol. Process.* **18**: 3401–3413.

Sighomnou D, Descroix L, Genthon P, Mahé G, Moussa IB, Gautier E, Mamadou I, Vandervaere JP, Bachir T, Coulibaly B, Rajot JL, Malam-Issa O, Malam-Abdou M, Dessay N, Delaitre E, Faran-Maiga O, Diedhiou A, Panthou G, Vischel T, Yacouba H, Karambiri H, Paturel JE, Diello P, Mougin E, Kergoat L, Hiernaux P. 2013. La crue de 2012 a Niamey: un paroxysme du paradoxe du Sahel? *Sécheresse* **24**: 3–13.

WMO, 2012. *Standardized precipitation index user guide* (M. Svoboda, M. Hayes and D. Wood), WMO. Geneva.